



HAL
open science

DFT Study of the Formation of Atmospheric Aerosol Precursors from the Interaction between Sulfuric Acid and Benzenedicarboxylic Acid Molecules

Bastien Radola, Sylvain Picaud, Ismael Kenneth Ortega

► **To cite this version:**

Bastien Radola, Sylvain Picaud, Ismael Kenneth Ortega. DFT Study of the Formation of Atmospheric Aerosol Precursors from the Interaction between Sulfuric Acid and Benzenedicarboxylic Acid Molecules. *Journal of Physical Chemistry A*, 2022, 126 (7), pp.1211-1220. 10.1021/acs.jpca.1c08936 . hal-03566581

HAL Id: hal-03566581

<https://hal.science/hal-03566581>

Submitted on 6 Oct 2022

HAL is a multi-disciplinary open access archive for the deposit and dissemination of scientific research documents, whether they are published or not. The documents may come from teaching and research institutions in France or abroad, or from public or private research centers.

L'archive ouverte pluridisciplinaire **HAL**, est destinée au dépôt et à la diffusion de documents scientifiques de niveau recherche, publiés ou non, émanant des établissements d'enseignement et de recherche français ou étrangers, des laboratoires publics ou privés.

A DFT Study of the Formation of Atmospheric Aerosol Precursors from the Interaction Between Sulfuric Acid and Benzenedicarboxylic Acid Molecules

Bastien Radola,[†] Sylvain Picaud,^{*,†} and Ismaël Kenneth Ortega^{*,‡}

*[†]Institut UTINAM – UMR 6213, CNRS / Université de Bourgogne Franche-Comté,
F-25030 Besançon Cedex, France*

*[‡]Multi-Physics for Energetics Department – ONERA / Université Paris Saclay, F-91123
Palaiseau, France*

E-mail: sylvain.picaud@univ-fcomte.fr; ismael.ortega@onera.fr

Abstract

Dicarboxylic acids are ubiquitous products of the photo-oxidation of volatile organic compounds which are believed to play a significant role in the formation of secondary organic aerosols in the atmosphere. In this paper, we report high-level quantum investigations of the clustering properties of sulfuric acid and benzenedicarboxylic acid molecules. Up to four molecules have been considered in the calculations and the behavior of the three isomers of the organic diacid species have been compared. The most stable geometries have been characterized together with the corresponding thermodynamic data. From an atmospheric point of view, the results of the DFT calculations show that the organic diacid molecules may significantly enhance the nucleation of small atmospheric clusters, at least from an energetic point of view. In this respect, the phthalic acid isomer seems more efficient than the two other isomers of the benzenedicarboxylic acid, in particular because the internal distance between the two carboxyl groups in the organic diacids appears to play an important role in the stabilization of the H-bond network inside the corresponding heterocluster formed with sulfuric acid molecules.

Introduction

Organic aerosols (OAs) comprise an important, but still ill-characterized, fraction of atmospheric aerosols.¹⁻³ OAs may strongly impact on climate forcing through their radiative properties and their propensity to act as cloud condensation nuclei (CCN).^{2,4,5} They contribute to visibility degradation in strongly polluted areas⁶ where they are also suspected to have adverse effects on human health, arising from their small size and chemical composition.^{7,8} OAs can be either directly emitted into the atmosphere as primary particles (*e.g.*, from fossil fuel combustion and biomass burning)^{9,10} or produced *in situ* by the oxidation of various organic compounds originating both from anthropogenic and natural sources. In this last case, they form what is called secondary organic aerosols (SOAs).^{11,12} Unfortu-

nately, despite the recent recognition of OAs as major players of the Earth’s atmosphere, the huge variety of these SOAs, which may represent up to 40 % of the OA fraction, strongly limits our knowledge of their properties and environmental impacts.^{13–15} Thus, SOAs are the subject of a growing number of research studies, combining field observations, experimental characterization and numerical modeling, aiming at better characterizing not only their chemical composition but also their atmospheric transformation and fate.¹⁶ A focus is especially made on the atmospheric formation mechanism of SOAs from the clustering of different gas phase molecules, which appears to be a complex process,⁵ initiated via the collision of organic species that stay stuck together via intermolecular interactions, including chemical bonding, hydrogen-bonding, coulombic and/or van de Waals interactions.^{17–19} The small clusters formed this way may grow and become stable against evaporation of their constituents, thus reaching the critical size.²⁰ Additional uptake of gases, again via more or less strong intermolecular interactions, may then spontaneously lead to subsequent growth up to detectable sizes.¹⁷ Concomitantly, these newly formed clusters may also be scavenged by various processes including coagulation with pre-existing particles and rain precipitation, which limits their lifetime in the atmosphere.¹⁸

Thanks to the development of cutting edge experiments, our knowledge on the first steps of the aerosol nucleation has deeply improved during recent years.^{18,21} Thus, it is now well recognized that new-particle formation likely involves sulfuric acid (SA) and that only very few SA molecules might be involved in the formation of the corresponding critical nuclei, especially if other species like highly oxidized organic compounds are simultaneously present.^{17,18,22–28} As a consequence, molecular nuclei relevant for atmospheric nucleation may be very small,¹⁸ allowing a molecular-level characterization of their formation on the basis of quantum chemistry methods as, for instance, the density functional theory (DFT).²⁹ Thus, various numerical approaches of the corresponding pre-nucleation mechanisms have recently focused on the properties of clusters made of different species,^{19,20,29–34} also leading to the recent publication of a compiled database consisting of more than 630 atmospherically rel-

evant clusters.³³ Organic acids have been especially considered in these theoretical studies, because experimental evidence suggests that they play a key role in the initial nucleation of particles together with the SA molecules.²² This feature has been associated with the ability of the carboxyl groups to form strong hydrogen bonds with the surrounding sulfuric acid molecules.^{30,32} Among these organic acids, low molecular weight (LMW) dicarboxylic acids are of special interest because they represent the most abundant class of organic compounds in aerosols.¹⁵ In addition, their high water-solubility and hygroscopic properties may enhance the ability of the corresponding aerosol particles to act as CCN or ice nuclei. As a consequence, atmospheric LMW dicarboxylic acids might directly impact on the Earth radiative balance.³⁵

LMW dicarboxylic acids are rarely produced as primary compounds but rather, result from complex photochemical oxidation reactions of various organic precursors.¹⁵ Oxalic acid is generally the most abundant dicarboxylic acid in the atmosphere, followed by malonic and succinic acids.^{15,35-37} Besides these aliphatic acid molecules, benzenedicarboxylic acid ($C_8H_6O_4$) is also broadly present in ambient aerosols,³⁸⁻⁴⁰ mainly originating from the oxidation of naphthalene, benz[a]anthracene and other polycyclic aromatic hydrocarbons that can be produced in diesel exhaust, coal combustion and biomass burning.³⁸ Benzenedicarboxylic acid has been also found in emissions collected in aircraft engine exhaust running at low thrust.⁴¹ Thus, benzenedicarboxylic acid has been proposed as a surrogate for the contribution of SOA to an ambient sample, arising from naphthalene, methyl-naphthalene, and possibly other 2-ring, gas-phase PAHs, in a source attribution approach.⁴² However, this aromatic diacid may also be emitted from primary sources such as off-gassing of plasticizers from plastics, which complexifies any source attribution.⁴³ Note that, from a molecular point of view, the three *o*-, *m*-, *p*- $C_8H_6O_4$ isomers, usually called phthalic (PA), isophthalic (iPA) and terephthalic (tPA) acid molecules (Fig. 1) have been detected in aerosol samples, with however different abundances suggesting different origins.^{36,39,40}

Although the interaction of benzenedicarboxylic acid with SA has been recently inves-

tigated by means of DFT approaches using various functionals and basis sets,^{30,32,44} the corresponding studies have been restricted to either one phthalic acid molecule interacting with one³² or two³⁰ SA molecules, or to the characterization of the bimolecular clusters formed by one SA molecule and one molecule of each of the $C_8H_6O_4$ isomers.⁴⁴ Moreover, the conclusions concerning the structure and the thermodynamics of the most stable clusters obtained in these theoretical studies are somehow different, depending on the methodology used in the quantum approaches. As a consequence, here, we follow a numerical procedure similar to the one used in our previous study devoted to skatole oxidation products,⁴⁵ to go one step further by characterizing the pre-nucleation hetero-clusters formed between the three *o*-, *m*-, *p*- $C_8H_6O_4$ isomers and up to three SA molecules (*i.e.*, up to four molecules are considered in the optimized clusters). In particular, the most stable clusters are identified via preliminary optimization at a semi-empirical level, followed by subsequent DFT optimizations performed on selected configurations. The energy, enthalpy and Gibbs free energy of formation of these clusters are then calculated at the same level of theory. Note that considering the three $C_8H_6O_4$ isomers simultaneously in the same study allows a careful investigation of the influence of the carboxyl groups position on the clustering capacity of these organic acid molecules. In addition, the results obtained for the heteroclusters are compared to those obtained for homoclusters made of either SA molecules or benzenedicarboxylic acid molecules, only, in particular because it is known that highly oxidized organic compounds on their own can form new particles in the atmosphere without sulfuric acid.²⁷

The present paper is organized as follows. The computational details simulations are provided in Section 2 and the corresponding results for the cluster configurations are discussed in Section 3. Finally, the main conclusions of this study are summarized in section 4.

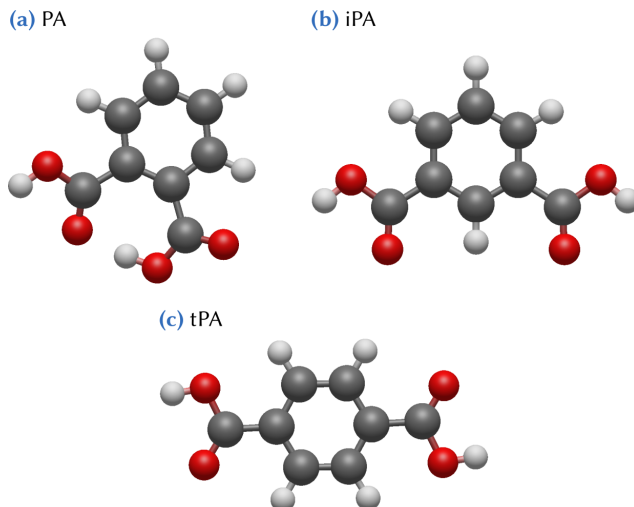


Figure 1: Snapshots of the (a) phthalic (PA), (b) isophthalic (iPA), and (c) terephthalic (tPA) isomers of the benzenedicarboxylic acid molecule considered in this work. These geometries have been optimized at the ω B97X-D/6-31++G(d,p) level of theory. Hydrogen, carbon, and oxygen atoms are represented in white, dark gray, and red, respectively.

Computational Details

The optimization of the different clusters considered in this study has followed a procedure previously used in a similar context.⁴⁵ First, a set of initial conformers has been semi-randomly generated by placing one SA molecule around one benzenedicarboxylic acid molecule or one previously formed small cluster, in preferential regions selected because of their strong electrostatic charge, as identified by generating electrostatic potential maps using the NPA method.⁴⁶ Indeed, proceeding this way has ensured that only the regions of the configuration space that most likely lead to strong binding have been sampled. Between 30 and 240 configurations have been generated this way for each system under consideration, which have then been pre-optimized, first, at the semi-empirical PM6 and, afterwards, at the PW91/6-31G(d,p) levels of theory.

Once this pre-optimization has been completed, the resulting conformers have been sorted by their electronic energy and the lowest energy configurations, within 8 kcal mol^{-1} , have been selected for further optimization at the ω B97X-D/6-31++G(d,p) level of theory. The ω B97X-D exchange-correlation functional used in these calculations is a long-range corrected

hybrid functional which includes dispersion corrections.⁴⁷ It has been selected on the basis of previous studies showing that ω B97X-D has performed slightly better than other functionals to estimate the energies of a set of 11 small atmospheric relevant clusters, when compared to calculations performed with CCSD(T) complete basis set.⁴⁸

The corresponding calculations have been performed with a dense integration grid (ultra-fine) and tight convergence criteria, together with a vibrational frequency analysis. The latter has allowed us, first, to ensure that the obtained geometry has a proper energy minimum and, second, to compute the thermodynamic quantities at standard conditions (*i.e.*, $T = 298.15$ K and $P = 1$ atm) using the rigid-rotor harmonic oscillator approximation, with a quasi-harmonic treatment for the low-lying frequency modes.^{49,50} The optimized configurations have been carefully analyzed to discard highest energy conformers, within 6 kcal mol^{-1} , and redundant configurations. Finally, to obtain a better evaluation of the electronic energy, a single-point calculation at the ω B97X-D/def2-TZVPPD level of theory has been carried out on top of the most stable geometries optimized at the ω B97X-D/6-31++G(d,p) level of theory. The Gaussian 09 quantum chemistry software⁵¹ has been used for all calculations.

Computed thermodynamic quantities have been the binding energy, ΔE , corrected by the zero-point vibration energy, the enthalpy of formation, ΔH , and the Gibbs energy of formation, ΔG . In these calculations, the following definition has been used:

$$\Delta\Theta = \Theta[n \text{ xPA} + m \text{ SA}] - n\Theta[\text{xPA}] - m\Theta[\text{SA}] \quad (1)$$

where Θ denotes either the energy, E , the enthalpy, H , or the Gibbs energy, G , and xPA refers to the various isomers of the benzenedicarboxylic acid (*i.e.*, PA, iPA and tPA). In addition, when considering the formation of clusters made of n benzenedicarboxylic acid molecules and more than one SA molecule ($m > 1$), three alternative definitions for the

calculation of these thermodynamic quantities have been considered, namely:

$$\Delta\Theta^* = \Theta[n \text{ xPA} + m \text{ SA}] - \Theta[n \text{ xPA} + (m-1) \text{ SA}] - \Theta[\text{SA}] \quad (2)$$

$$\Delta\Theta^\dagger = \Theta[n \text{ xPA} + m \text{ SA}] - \Theta[n \text{ xPA} + (m-2) \text{ SA}] - \Theta[2 \text{ SA}] \quad (3)$$

$$\Delta\Theta^\ddagger = \Theta[n \text{ xPA} + m \text{ SA}] - \Theta[n \text{ xPA} + (m-3) \text{ SA}] - \Theta[3 \text{ SA}] \quad (4)$$

which correspond to different pathways for the cluster formation (*i.e.*, the direct addition of one, two or three SA molecules, respectively) to an already preformed cluster made of xPA and SA molecules.

Note that additional optimizations have also been performed at the $\omega\text{B97X-D/aug-pcseg-1}$ and $\omega\text{B97X-D/def2-SVPD}$ levels of theory, for comparison with the results obtained at the $\omega\text{B97X-D/6-31++G(d,p)}$ level of theory. As in our previous study,⁴⁵ the geometries optimized with these three methods have been found to be very similar, with a mean bond length deviation, including hydrogen bonds, equal or lower than 2×10^{-2} Å. However, energy differences have been found to be more pronounced than geometry differences, even if it has not resulted in a dramatic change of the ordering of the configurations. Additionally, some geometries optimized at the $\omega\text{B97X-D/aug-pcseg-1}$ and $\omega\text{B97X-D/def2-SVPD}$ levels of theory have been subjected to $\omega\text{B97X-D/def2-TZVPPD}$ single-point calculations. Due to the small geometry differences between the three double- ζ basis set optimizations, the energy deviation has been found to be quite small, with a maximum of 2×10^{-1} kcal mol⁻¹ difference. Moreover, zero-point vibration energy, enthalpy and entropy corrections, also calculated at the $\omega\text{B97X-D/aug-pcseg-1}$ and $\omega\text{B97X-D/def2-SVPD}$ levels of theory, have been found to be quite similar to those obtained at the $\omega\text{B97X-D/6-31++G(d,p)}$ level of theory, with a mean energy deviation of about 3×10^{-1} kcal mol⁻¹. This has confirmed that a full optimization at the $\omega\text{B97X-D/6-31++G(d,p)}$ level of theory with an additional single-point calculation using a triple- ζ basis set can be considered sufficiently accurate for the systems under investigation here. As a consequence, only the results obtained with this approach will be discussed in

detail below.

Results and Discussion

Dimers of Benzenedicarboxylic and Sulfuric Acid Molecules

The structures of the lowest energy dimers made of one SA molecule and one molecule of each of the benzenedicarboxylic acid isomers (*i.e.*, PA, iPA and tPA) are shown in Fig. 2 and the corresponding thermodynamic data are given in Table 1.

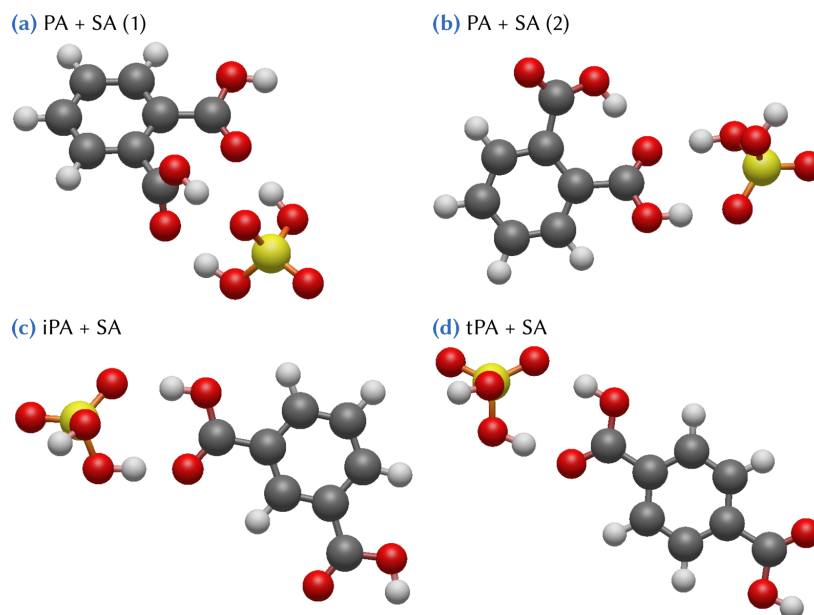


Figure 2: Snapshots of the most stable configuration obtained for a dimer made of one sulfuric acid and one (a,b) phthalic, or one (c) isophthalic, or one (d) terephthalic molecule, as obtained from DFT calculations at the ω B97X-D/6-31++G(d,p) level of theory. Hydrogen, carbon, oxygen and sulfur atoms are represented in white, dark gray, red and yellow, respectively.

Let us first comment the most stable structures which have been optimized when considering the iPA and tPA molecules (Figs. 2c and d), because they are very similar and, thus, correspond to almost equivalent thermodynamic results (Table 1). Indeed, in both cases, the SA molecule form a pair of one donor and one acceptor hydrogen bonds with one of the two carboxyl groups of the benzenedicarboxylic acid molecule which, in these isomers, are

Table 1: Energetic data obtained from single-point calculations at the ω B97X-D/def2-TZVPPD level of theory, on top of a geometry optimized at the ω B97X-D/6-31++G(d,p) level of theory. Thermal contributions and zero-point vibration energy were evaluated at the ω B97X-D/6-31++G(d,p) level of theory. All values are given in kcal mol⁻¹.

Configurations	ΔE	ΔH	ΔG	ΔG^*	ΔG^\dagger	ΔG^\ddagger
PA + SA (1)	-21.1	-21.9	-8.8	—	—	—
PA + SA (2)	-15.3	-16.2	-3.7	—	—	—
iPA + SA	-17.9	-18.9	-6.1	—	—	—
tPA + SA	-17.5	-18.6	-5.8	—	—	—
(PA) ₂	-13.9	-14.9	-1.8	—	—	—
PA + iPA	-16.2	-17.3	-4.0	—	—	—
PA + tPA	-15.9	-16.9	-3.7	—	—	—
(iPA) ₂	-17.5	-18.5	-5.1	—	—	—
iPA + tPA	-17.2	-18.2	-4.8	—	—	—
(tPA) ₂	-16.9	-18.0	-4.5	—	—	—
PA + 2 SA (1)	-39.0	-41.0	-13.4	-4.5	-8.2	—
PA + 2 SA (2)	-34.9	-36.9	-9.3	-0.4	-4.1	—
iPA + 2 SA	-35.3	-37.4	-11.6	-5.5	-6.4	—
tPA + 2 SA	-34.9	-37.0	-11.4	-5.6	-6.2	—
PA + 3 SA (1)	-58.1	-61.2	-19.5	-6.2	-5.5	-10.1
PA + 3 SA (2)	-55.0	-58.1	-16.4	-3.1	-2.4	-6.9
iPA + 3 SA (1)	-52.7	-55.9	-16.3	-4.6	-4.9	-6.8
iPA + 3 SA (2)	-53.9	-57.1	-15.8	-4.2	-4.5	-6.3
tPA + 3 SA	-52.1	-55.3	-15.5	-4.1	-4.5	-6.1
2 PA + SA	-42.0	-43.7	-15.4	-13.5	—	—
2 iPA + SA	-35.5	-37.6	-11.1	-6.0	—	—
2 tPA + SA	-35.0	-37.1	-11.2	-6.7	—	—
(SA) ₂	-16.4	-17.5	-5.2	—	—	—
(SA) ₃	-32.4	-34.5	-9.5	-4.3	—	—
(SA) ₄	-50.2	-53.4	-13.0	-3.5	-2.6	—

located sufficiently far apart for not being simultaneously involved in the bonding with SA. The corresponding Gibbs free energy calculated following the procedure described above (Eq. (1)) are equal to -6.1 and $-5.8 \text{ kcal mol}^{-1}$ for the iPA + SA and tPA + SA dimers, respectively. Note that because of the separation between the two carboxyl groups in these iPA and tPA isomers, their corresponding dimers with SA have been quite easily optimized and, thus, no other conformer has been found in our investigations. These structures are very similar to those recently obtained with the PW91 and the M06-2X functionals and the 6-311++G(d,p) basis set, although in this case, the corresponding Gibbs free energies are slightly lower, ranging from -7.9 to $-7.3 \text{ kcal mol}^{-1}$, depending on the method used.⁴⁴

The situation is a bit different when considering the phthalic acid isomer in which the two carboxyl groups are sufficiently close together to form a strong intramolecular hydrogen bond. Indeed, in this case, two stable conformers have been evidenced. In the first one, SA is tied to the PA molecule by two H-bonds formed with only one of the two carboxyl groups of the PA molecule (Fig. 2b), thus keeping intact its intramolecular hydrogen bond. The corresponding geometry is in fact very similar to those optimized when considering the iPA and tPA isomers of benzenedicarboxylic acid (Figs. 2c and d). Note that only this configuration has been found in previous studies using the PW91 and the M06-2X functionals together with the 6-311++G(d,p) basis set, with Gibbs free energy being equal to -4.47 and $-5.26 \text{ kcal mol}^{-1}$, respectively.⁴⁴ The calculations performed here at the ω B97X-D/def2-TZVPPD level of theory has led to a slightly higher value of $-3.7 \text{ kcal mol}^{-1}$. Anyway, this configuration can be viewed as a local minimum only, because a much more stable structure has been found when allowing the breaking of the intramolecular hydrogen bond of the PA molecule. Indeed, this has led to the formation of three hydrogen bonds with the SA molecule, two of them being donor H-bonds, while the third one corresponds to the formation of an acceptor H-bond between one oxygen atom and one $-\text{OH}$ group of the SA and PA molecules, respectively (Fig. 2a). The Gibbs free energy of this structure is equal to $-8.8 \text{ kcal mol}^{-1}$, the energy loss (in absolute value) resulting from the breaking of the intramolecular H-bond

of the PA molecule being more than compensated by the corresponding energy gain due to the formation of the third intermolecular H-bond with the SA molecule. This configuration is very similar to the one previously optimized at the M06-2X/6-31++G(d,p) level of theory and the Gibbs free energy value obtained in the present work is exactly the same as previously obtained by performing high-level CCSD(T)-F12a/VDZ-F12 calculations.⁵²

It is worth mentioning that, from a thermodynamic point of view, the present results indicate that the formation of an heterodimer made of one xPA acid and one SA molecules always appears favored with respect to the formation of the SA dimer (the free energy values for the formation of these dimers are equal to -8.8 , -6.1 , and -5.8 kcal mol⁻¹, for PA + SA, iPA + SA and tPA + SA, respectively, vs -5.2 kcal mol⁻¹ for (SA)₂, see Table 1). It is also energetically favored when compared to the formation of any benzenedicarboxylic acid dimer, irrespective of the isomer considered (see Fig. 3 and Table 1 for the optimized geometries and the corresponding free energies of these acid dimers, respectively). Indeed, among all the possibilities, the lowest Gibbs free energy value (-5.1 kcal mol⁻¹), which is calculated for the formation of the (iPA)₂ dimer, still remains 1.0 kcal mol⁻¹ higher than the corresponding value for the iPA + SA dimer (Table 1). Of course, such a conclusion does not take into account any kinetic arguments nor any probability of occurrence, which may depend on the relative atmospheric concentrations of these various species.⁴⁴

Beyond the Dimers

Heteroclusters made of one xPA and two or three SA molecules have been optimized at the level of theory detailed above. The corresponding thermodynamic results are given in Table 1 while the most stable configurations which have been optimized with our approach are shown in Figs. 4 and 5. First, when considering the optimized structures for the various xPA + 2SA trimers, it can be easily seen that the two SA molecules are attached to the two carboxyl group of the iPA and tPA molecules, without evidence for any bonding between the SA molecules themselves. This is confirmed by the fact that the corresponding ΔE values

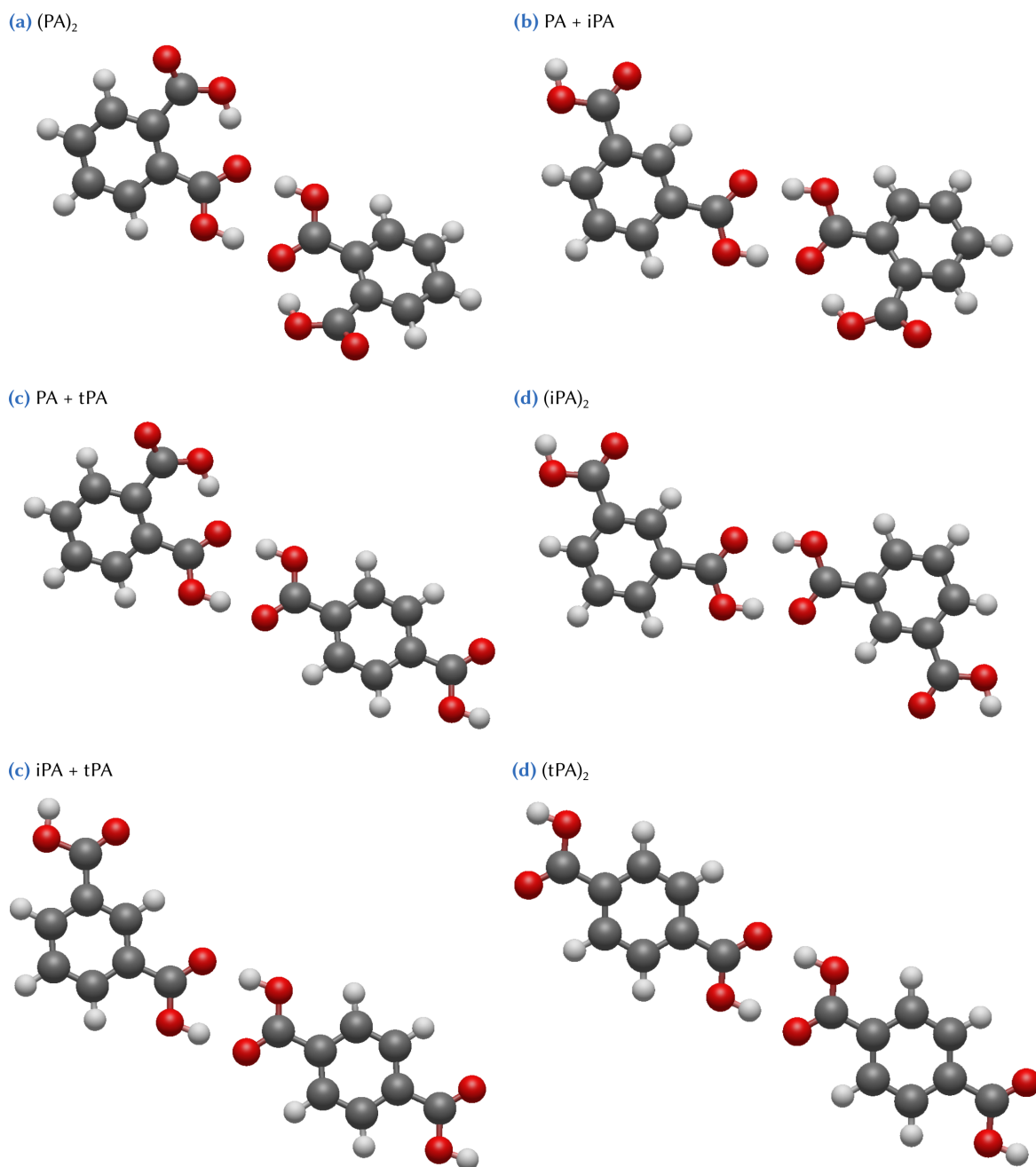


Figure 3: Geometries of the xPA dimers optimized at the ω B97X-D/6-31++G(d,p) level of theory. Hydrogen, carbon, oxygen and sulfur atoms are represented in white, dark gray, red, and yellow, respectively.

are roughly twice those calculated for the iPA + SA and tPA + SA dimers. Moreover, for both systems, the addition of the second SA molecule corresponds to the similar free energy change of about $-5.5 \text{ kcal mol}^{-1}$, as indicated by the corresponding values of ΔG^* . The situation is, again, a bit different when looking at the behavior of the PA molecule. Indeed, in this case, two stable configurations are evidenced in the calculations, with free energy values equal to -13.4 and $-9.3 \text{ kcal mol}^{-1}$, corresponding to the breaking (Fig. 4a) and the preservation (Fig. 4b) of the intramolecular hydrogen bond in the PA molecule, respectively. It is interesting to note that the trimer which has the lowest free energy of formation appears strongly stabilized by the formation of two H-bonds between the SA molecules, whereas only one is formed in the other configuration. Thus, the energy change related to the breaking of the intramolecular H-bond of the PA molecule appears compensated by the formation of a second H-bond between the two attached SA molecules. For the most stable configuration of the PA + 2SA trimer, the addition of one SA molecule corresponds to a net free energy change (ΔG^*) of $-4.5 \text{ kcal mol}^{-1}$ with respect to the most stable PA + SA dimer.

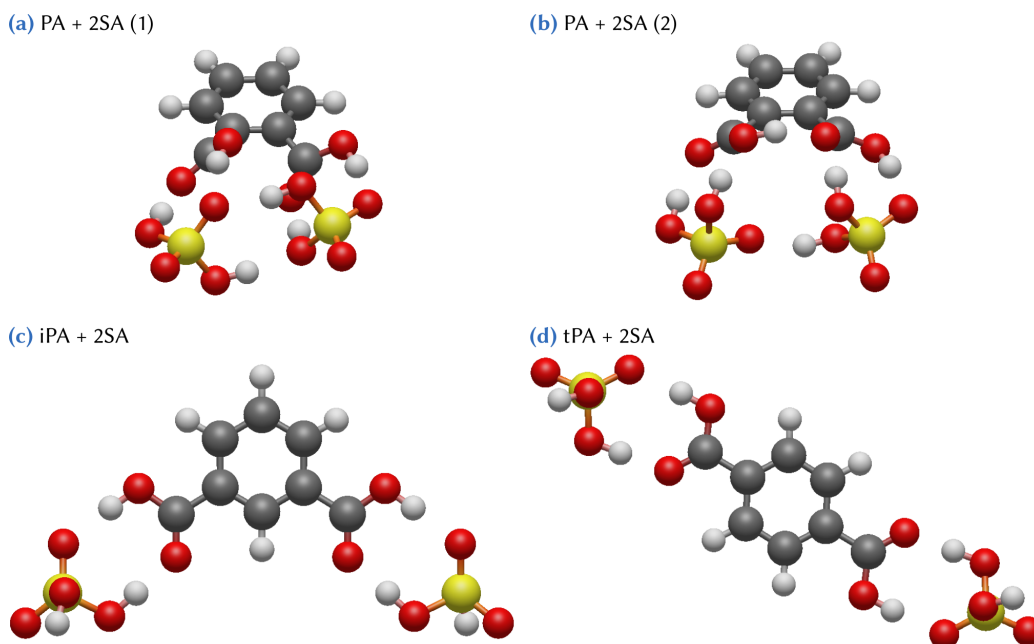


Figure 4: Geometries of the xPA + 2SA clusters optimized at the ω B97X-D/6-31++G(d,p) level of theory. Hydrogen, carbon, oxygen and sulfur atoms are represented in white, dark gray, red, and yellow, respectively.

The stable configurations obtained when three SA molecules interact with one xPA molecule are shown in Fig. 5. For these tetramers, two different situations are evidenced, depending on the distance between the two carboxyl groups in the xPA molecules. Indeed, two of the three attached SA molecules optimize their H-bonding with the two distant carboxyl groups of the tPA molecule, while the third SA molecule is directly tied to one of the two others (Fig. 5e). Such a configuration is also found on the iPA molecule (Fig. 5c), although a second, slightly less stable, minimum is also found, in which the three SA molecules rather tend to optimize their intermolecular H-bonding (Fig. 5d). It is interesting to note that although the latter has a lower energy of formation than the former (-53.9 *vs.* -52.7 kcal mol $^{-1}$), the reverse situation prevails with regards to the Gibbs free energy of formation (-15.8 *vs.* -16.3 kcal mol $^{-1}$) due to entropic effects. Moreover, when considering the PA molecule for which the two carboxyl groups are close together, the three attached SA molecules tend to optimize their H-bonding both with the PA molecule and between themselves. In this situation, two energy minima are evidenced, the most stable configuration (Fig. 5a) being related to the breaking of the intramolecular H-bond of the PA molecule ($\Delta G = -19.5$ kcal mol $^{-1}$), whereas in the second, less stable, configuration (Fig. 5b), this intramolecular H-bond remains almost preserved ($\Delta G = -16.4$ kcal mol $^{-1}$). As already observed for the smaller clusters, the breaking of the intramolecular H-bond in the PA molecule allows the formation of one additional intermolecular H-bond with the SA molecules, the energy gain (in absolute value) associated with the formation of the latter compensating for the energy loss corresponding to the breaking of the former. Also, it is worth mentioning that although proton transfer has been sometimes observed during the optimization procedure, the Gibbs free energy of formation of the corresponding structures has always been found higher than the one of the stable structures detailed above. This indicates that the clustering of the molecules considered here remains likely a process involving non-dissociated molecular species, only.

From a thermodynamic point of view, the present results show that the formation of an heterocluster made of one xPA and two or three SA molecules always appears favored with

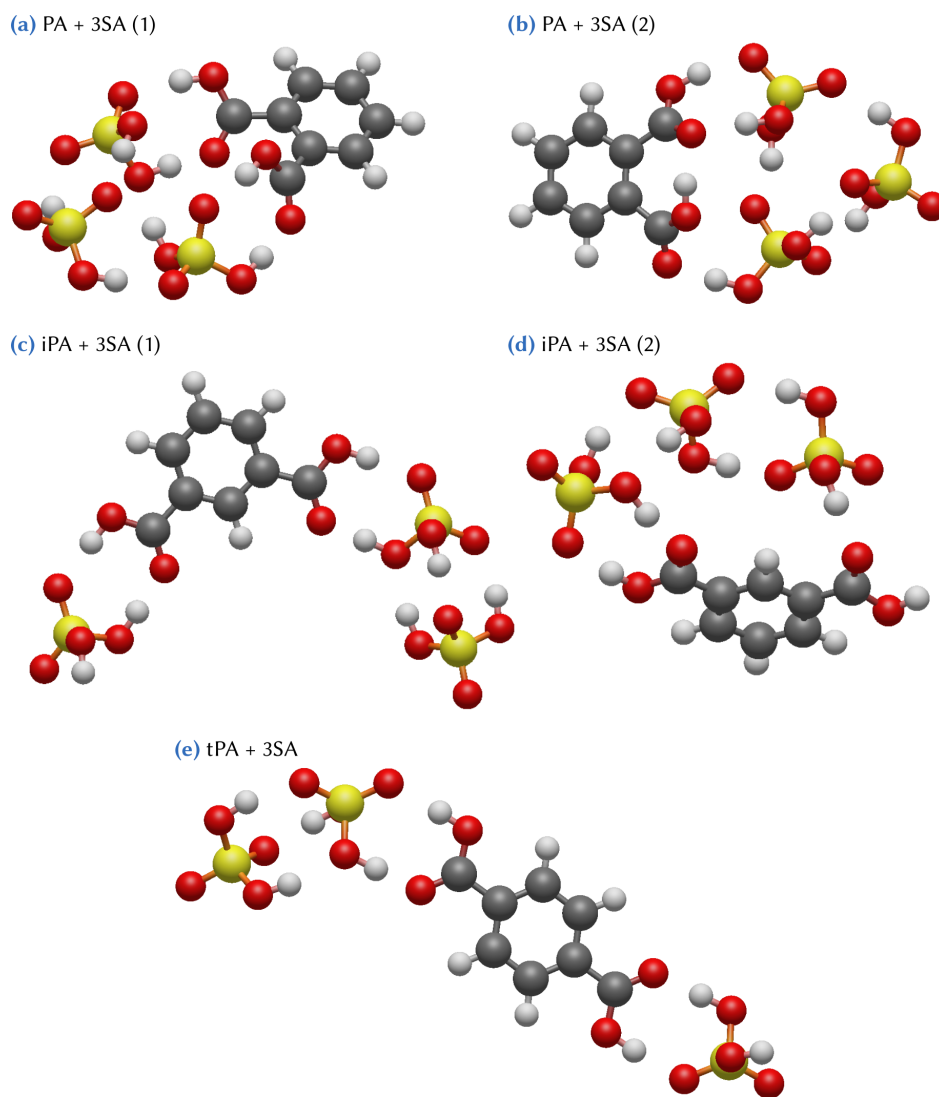


Figure 5: Geometries of the xPA + 3SA clusters optimized at the ω B97X-D/6-31++G(d,p) level of theory. Hydrogen, carbon, oxygen and sulfur atoms are represented in white, dark gray, red, and yellow, respectively.

respect to the formation of the SA trimer or the SA tetramer (see the corresponding ΔG values in Table 1). This clearly shows that the presence of the organic diacid may strongly favor the nucleation of the sulfuric acid molecules.

In addition, it appears that the 2PA + SA trimer has a lower Gibbs free energy of formation than any of the stable PA + 2SA clusters (the smallest energy difference being equal to 2 kcal mol^{-1} , see Table 1). This may be explained by a better optimization of the H-bonds network between the three molecules in the former case, although the same total number of 6 H-bonds is observed in the two situations (Fig. 6a). For the two other xPA isomers (iPA and tPA), the most stable 2xPA + SA and xPA + 2SA clusters (Figs. 6b,c) have very similar Gibbs free energy of formation (Table 1) and, from a thermodynamic point of view, their formation may thus appear equally likely. Again, these conclusions do not account for any kinetic arguments nor any relative atmospheric abundances of these various species, which may however control both their collision and sticking probabilities.

Finally, note that we did not try to optimize other molecular combinations for these heteroclusters (for instance, clusters made of more than two dicarboxylic acid molecules, or made of two xPA and two SA molecules) due to the increasing number of different possibilities and the numerical resources that would thus be required to find the absolute minimum for the corresponding structures.

Calculations of evaporation rates

Beside thermodynamical results, additional information on the cluster stability has been obtained from the calculation of the evaporation rates for the most stable clusters optimized above, following the procedure detailed by Ortega et al.⁵³ These evaporation rates have been determined at 298.15 K and 101 325 Pa. For each cluster we have considered all potential evaporation pathways, keeping then the one with the highest evaporation rate, only. For example, for the sulfuric acid tetramer, we have considered the evaporation of one monomer leading to the trimer and the evaporation of a dimer leading to a dimer. The corresponding

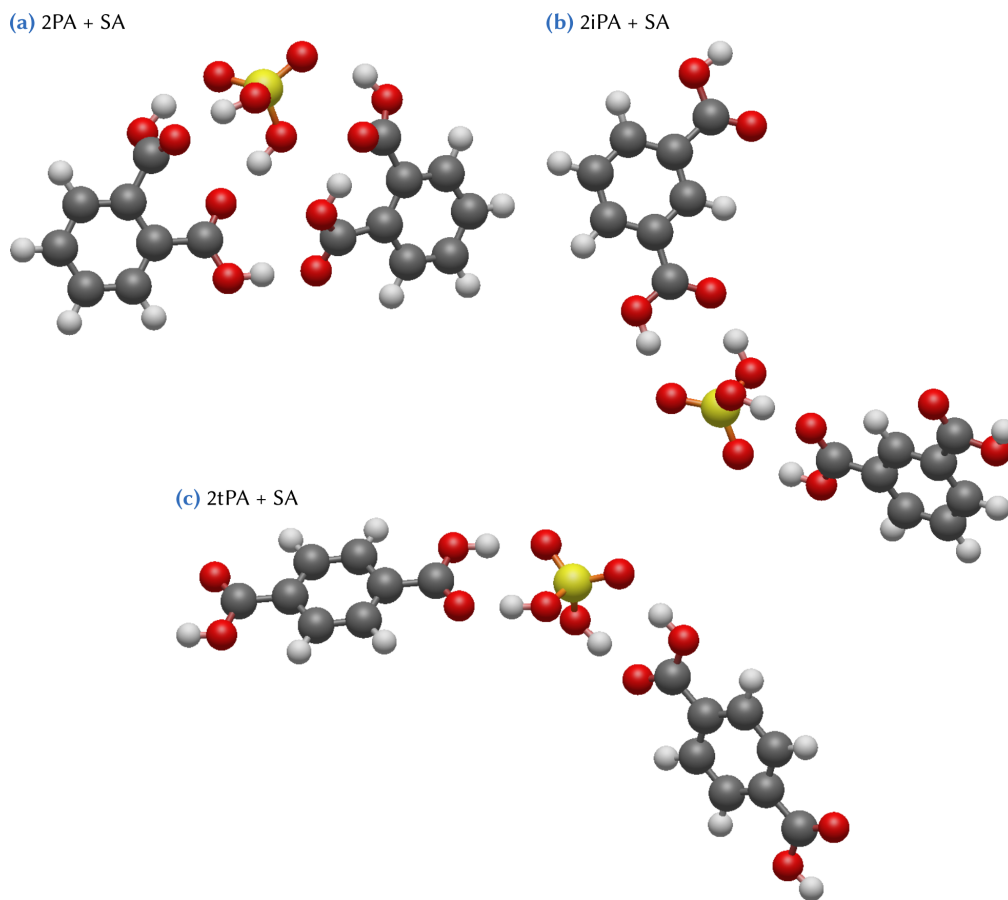


Figure 6: Geometries of the 2xPA + SA clusters optimized at the ω B97X-D/6-31++G(d,p) level of theory. Hydrogen, carbon, oxygen and sulfur atoms are represented in white, dark gray, red, and yellow, respectively.

results are given in Table 2.

From the evaporation rate point of view, we can see that the xPA + SA clusters have an evaporation rate significantly lower than the one calculated for the sulfuric acid dimer (this is especially true for the PA + SA dimer) and that those of the carboxylic acid dimers. Moreover, the addition of a second PA molecule to these clusters (*i.e.*, 2xPA + SA) seems more favorable than the addition of a second molecule of sulfuric acid (*i.e.*, xPA + 2SA), at least for PA and tPA acids. All the 2xPA + SA trimers also appear more stable than the sulfuric acid trimer. In addition, when considering tetramers, the evaporation rates show that adding a xPA molecule to the sulfuric acid trimer may strongly stabilize it, with respect to the addition of a fourth SA molecule. Thus, the analysis of these evaporation rates infers conclusions that are in line with those issued from the thermodynamic results. Of course, the precise pathways for clustering will as well depend on the concentration of both xPA and SA molecules. Further studies are thus necessary to confirm the exact role of xPA in new particle formation.

On the other hand, by definition, the values of the evaporation rates depend on the free energy values calculated for the formation of the clusters under investigation. Unfortunately, for large clusters, no method can ensure that the global minimum free-energy has actually been found in the calculations. However, the present results represent at least a lower limit for the cluster stability, because discovering better structures (*i.e.*, structures corresponding to a lower free energy value) would only lead to lower evaporation rates, thus even more stable clusters. As the pure sulfuric acid clusters have been extensively explored in the literature, preventing thus better structures to be found, any benzenedicarboxylic acid cluster more stable than those found here, would then reinforce our conclusions on the stabilization effect of these molecules when compared to the pure SA clusters.

Table 2: Evaporation rates (s^{-1}) for different clusters included in this work. The corresponding free energy of formation (kcal mol^{-1}), calculated at the $\omega\text{B97X-D/def2-TZVPPD}$ level of theory, is recalled.

Configurations	ΔG	evaporation rate
Dimers		
PA + SA	-8.8	3.40×10^3
iPA + SA	-6.1	3.24×10^5
tPA + SA	-5.8	5.38×10^5
(PA) ₂	-1.8	4.98×10^8
PA + iPA	-4.0	1.19×10^7
PA + tPA	-3.7	1.98×10^7
(iPA) ₂	-5.1	1.86×10^6
iPA + tPA	-4.8	3.09×10^6
(tPA) ₂	-4.5	5.13×10^6
(SA) ₂	-5.2	1.31×10^6
Trimers		
PA + 2 SA	-13.4	4.48×10^6
iPA + 2 SA	-11.6	9.80×10^5
tPA + 2 SA	-11.4	8.28×10^5
2 PA + SA	-15.4	1.53×10^5
2 iPA + SA	-11.1	2.28×10^6
2 tPA + SA	-11.2	5.91×10^5
(SA) ₃	-9.5	6.63×10^6
Tetramers		
PA + 3 SA	-19.5	9.40×10^5
iPA + 3 SA	-16.3	4.76×10^6
tPA + 3 SA	-15.5	5.09×10^6
(SA) ₄	-13.0	1.19×10^8

Conclusions

DFT calculations have been applied to investigate the interaction of the three benzenedicarboxylic acid isomers (PA, iPA, and tPA) with sulfuric acid, which is a common atmospheric aerosol nucleation precursor. Heteroclusters of up to four molecules have been considered and their most stable geometries have been characterized together with the corresponding thermodynamic data. When considering the Gibbs free energy of formation, our results show that the clusters optimized when considering interaction of sulfuric acid molecules with the iPA or tPA isomers are characterized by roughly the same values, and are always less stable than those formed with the phthalic acid isomer, provided that the intramolecular H-bond in this PA isomer is broken. This conclusion is obtained irrespective of the number of SA molecules considered in the calculations and it can be related to the internal distance between the two carboxyl groups in the organic acid molecules. Indeed, when the $-\text{COOH}$ groups are in the ortho position (PA), their proximity allows for the formation of additional H-bonds between the attached sulfuric acid molecules, thus reinforcing the H-bond network inside the corresponding heterocluster. These results nicely complement previous conclusions drawn from the examination of the interaction between various organic acid molecules and one sulfuric acid molecule.^{45,52} They also confirm that the intramolecular hydrogen bond in the phthalic acid isomer has to be broken to enhance the interaction with sulfuric acid molecule,³² a feature which seems however not obtained in some other studies using a different quantum chemistry level of theory.⁴⁴

More important from an atmospheric point of view, the present results show that the formation of an heterocluster made of benzenedicarboxylic and sulfuric acid molecules is always energetically favored with respect to the clustering of sulfuric acid molecules alone. When compared with the available results in the literature obtained with similar DFT approaches, it appears that the heterocluster based on benzenedicarboxylic acid molecules are also energetically more stable than those formed with other diacid molecules.^{30,44} Besides, the calculated evaporation rates also confirm that the addition of a benzenedicarboxylic acid

molecule may stabilize sulfuric acid clusters. These features thus infer that benzenedicarboxylic acid molecules may enhance the nucleation of small atmospheric clusters, as already discussed for other organic diacid molecules,³⁰ although they are certainly less efficient than bases which are known to strongly bind to sulfuric acid molecules.⁵⁴

Conflicts of interest

There are no conflicts to declare.

Supporting Information

Includes the cartesian coordinates and the thermodynamic data for all reported clusters.

This material is available free of charge via Internet at <http://pubs.acs.org>.

Acknowledgements

This work is supported by the UNREAL ANR-18-CE22-0019-03 project funded by the French ANR “*Agence Nationale de la Recherche*”. Calculations were performed using the computing resources of the *Mésocentre de Calcul*, a regional computing center at *Université de Franche-Comté*.

References

- (1) Jacobson, M. C.; Hansson, H. C.; Noone, K. J.; Charlson, R. J. Organic Atmospheric Aerosols : Review and State of the Science. *Reviews of Geophysics* **2000**, *38*, 267–294.
- (2) Kanakidou, M.; Seinfeld, J. H.; Pandis, S. N.; Barnes, I.; Dentener, F. J.; Facchini, M. C.; Dingenen, R. V.; Ervens, B.; Nenes, A.; et al., C. J. N. Organic Aerosol and Global Climate Modelling: a Review. *Atmos. Chem. Phys.* **2005**, *5*, 1053–1123.
- (3) Mahilang, M.; Deb, M. K.; Pervez, S. Biogenic Secondary Organic Aerosols: A Review on Formation Mechanism, Analytical Challenges and Environmental Impacts. *Chemosphere* **2021**, *262*, 127771.
- (4) Pöschl, U. Atmospheric Aerosols: Composition, Transformation, Climate and Health Effects. *Angew. Chem. Int. Ed.* **2005**, *44*, 7520–7540.
- (5) Fuzzi, S.; Andreae, M. O.; Huebert, B. J.; Kulmala, M.; Bond, T. C.; Boy, M.; Doherty, S. J.; Guenther, A.; Kanakidou, M.; et al., K. K. Critical Assessment of the Current State of Scientific Knowledge, Terminology, and Research Needs Concerning the Role of Organic Aerosols in the Atmosphere, Climate, and Global Change. *Atmos. Chem. Phys.* **2006**, *6*, 2017–2038.
- (6) Heal, M. R.; Kumar, P.; Harrison, R. M. Particles, Air Quality, Policy and Health. *Chem. Soc. Rev.* **2012**, *41*, 6606–6030.
- (7) Mauderly, J. L.; Chow, J. C. Health Effects of Organic Aerosols. *Inhal. Toxicol.* **2008**, *20*, 257–288.
- (8) Kim, K. H.; Kabir, E.; Kabir, S. A Review on the Human Health Impact of Airborne Particulate Matter. *Environ. Int.* **2015**, *74*, 136–143.
- (9) Kawamura, K.; Kaplan, I. R. Motor Exhaust Emissions as a Primary Source of

- Dicarboxylic-Acids in Los-Angeles Ambient Air. *Environ. Sci. Technol.* **1987**, *21*, 105–110.
- (10) Graham, B.; Mayol-Bracero, O. L.; Guyon, P.; Roberts, G. C.; Decesari, S.; Facchini, M. C.; Artaxo, P.; Maenhaut, W.; Koll, P.; Andreae, M. O. Water-Soluble Organic Compounds in Biomass Burning Aerosols Over Amazonia. 1. Characterization by NMR and GC-MS. *J. Geophys. Res.* **2002**, *107*, 8047.
- (11) Volkamer, R.; Jimenez, J. L.; Martini, F. S.; Dzepina, K.; Zhang, Q.; Salcedo, D.; Molina, L. T.; Worsnop, D. R.; Molina, M. J. Secondary Organic Aerosol Formation from Anthropogenic Air Pollution: Rapid and Higher than Expected. *Geophys. Res. Lett.* **2006**, *33*, L17811.
- (12) Shrivastava, M.; Cappa, C. D.; Fan, J.; Goldstein, A. H.; Guenther, A. B.; Jimenez, J. L.; Kuang, C.; Laskin, A.; Martin, S. T.; et al., N. L. N. Recent Advances in Understanding Secondary Organic Aerosol: Implications for Global Climate Forcing. *Reviews of Geophysics* **2017**, *55*, 509–559.
- (13) Goldstein, A. H.; Galbally, I. E. Known and Unexplored Organic Constituents in the Earth's Atmosphere. *Environ. Sci. Technol.* **2007**, *41*, 1514–1521.
- (14) Carslaw, K. S.; Boucher, O.; Spracklen, D. V.; Mann, G. W.; Rae, J. G. L.; Woodward, S.; Kulmala, M. A Review of Natural Aerosol Interactions and Feedbacks Within the Earth System. *Atmos. Chem. Phys.* **2010**, *10*, 1701–1737.
- (15) Kawamura, K.; Bikkina, S. A Review of Dicarboxylic Acids and Related Compounds in Atmospheric Aerosols: Molecular Distributions, Sources and Transformation. *Atmospheric Research* **2016**, *170*, 140–160.
- (16) Pandis, S. N.; Donahue, N. M.; Murphy, B. N.; Riipinen, I.; Fountoukis, C.; Karnezi, E.; Patoulias, D.; Skyllakou, K. Introductory Lecture: Atmospheric Organic Aerosols : In-

- sight from the Combination of Measurements and Chemical Transport Models. *Faraday Discussions* **2013**, *165*, 9–24.
- (17) Zhang, R. Getting to the Critical Nucleus of Aerosol Formation. *Science* **2010**, *328*, 1366–1367.
- (18) Zhang, R.; Khalizov, A.; Wang, I.; Hu, M.; Xu, W. Nucleation and Growth of Nanoparticles in the Atmosphere. *Chem. Rev.* **2012**, *112*, 1957–2011.
- (19) Myllys, N.; Olenius, T.; Kurtén, T.; Vehkamäki, H.; Riipinen, I.; Elm, J. Effect of Bisulfate, Ammonia, and Ammonium on the Clustering of Organic Acids and Sulfuric Acid. *J. Phys. Chem. A* **2017**, *121*, 4812–4824.
- (20) Elm, J. Toward a Holistic Understanding of the Formation and Growth of Atmospheric Molecular Clusters: A Quantum Machine Learning Perspective. *J. Phys. Chem. A* **2021**,
- (21) Kulmala, M.; Petäjä, T.; Ehn, M.; Thornton, J.; Sipilä, M.; Worsnop, D. R.; Kerminen, V. M. Chemistry of Atmospheric Nucleation : on the Recent Advances on Precursor Characterization and Atmospheric Cluster Composition in Connection with Atmospheric New Particle Formation. *Annu. Rev. Phys. Chem.* **2014**, *65*, 21–37.
- (22) Zhang, R.; Suh, I.; Zhao, J.; Zhang, D.; Fortner, E. C.; Tie, X.; Molina, L. T.; Molina, M. J. Atmospheric New Particle Formation Enhanced by Organic Acids. *Science* **2004**, *304*, 1487–1490.
- (23) Yue, D. L.; Hu, M.; Zhang, R. Y.; Wang, Z. B.; Zheng, J.; Wu, Z. J.; Wiedensohler, A.; He, L. Y.; Huang, X. F.; Zhu, T. The Roles of Sulfuric Acid in New Particle Formation and Growth in the Mega-City of Beijing. *Atmos. Chem. Phys.* **2010**, *10*, 4953–4960.
- (24) Kirkby, J.; Curtius, J.; Almeida, J.; Dunne, E.; Duplissy, J.; Ehrhart, S.; Franchin, A.; Gagné, S.; Ickes, L.; et al., A. K. Role of Sulphuric Acid, Ammonia and Galactic Cosmic Rays in Atmospheric Aerosol Nucleation. *Nature* **2011**, *476*, 429–433.

- (25) Riccobono, F.; Schobesberger, S.; Scott, C. E.; Dommen, J.; Ortega, I. K.; Rondo, L.; Almeida, J.; Amorim, A.; Bianchi, F.; et al., M. B. Oxidation Products of Biogenic Emissions Contribute to Nucleation of Atmospheric Particles. *Science* **2014**, *344*, 717–721.
- (26) Schobesberger, S.; Franchin, A.; Bianchi, F.; Rondo, L.; Duplissy, J.; Kürten, A.; Ortega, I. K.; Metzger, A.; Schnitzhofer, R.; et al., J. A. On the Composition of Ammonia-Sulfuric-Acid Ion Clusters During Aerosol Particle Formation. *Atmos. Chem. Phys.* **2015**, *15*, 55–78.
- (27) Kirkby, J.; Duplissy, J.; Sengupta, K.; Frege, C.; Gordon, H.; Williamson, C.; Heintz, M.; Simon, M.; Yan, C.; et al., J. A. Ion-Induced Nucleation of Pure Biogenic Particles. *Nature* **2016**, *533*, 521–526.
- (28) Kerminen, V. M.; Chen, X.; Vakkari, V.; Petäjä, T.; Kulmala, M.; Bianchi, F. Atmospheric New Particle Formation and Growth: Review of Field Observations. *Environ. Res. Lett.* **2018**, *13*, 103003.
- (29) Leonardi, A.; Ricker, H. M.; Gale, A. G.; Ball, B. T.; Odbadrakh, T. T.; Shields, G. C.; Navea, J. G. Particle Formation and Surface Processes on Atmospheric Aerosols : A Review of Applied Quantum Chemical Calculations. *Int. J. Quantum Chem.* **2020**, *120*, e26350.
- (30) Xu, W.; Zhang, R. Theoretical Investigation of Interaction of Dicarboxylic Acids with Common Aerosol Nucleation Precursors. *J. Phys. Chem. A* **2012**, *116*, 4539–4550.
- (31) Elm, J.; Fard, M.; Bilde, M.; Mikkelsen, K. V. Interaction of Glycine with Common Atmospheric Nucleation Precursors. *J. Phys. Chem. A* **2013**, *117*, 12990–12997.
- (32) Elm, J.; Myllys, N.; Olenius, T.; Halonen, R.; Kurtén, T.; Vehkamäki, H. Formation of Atmospheric Molecular Clusters Consisting of Sulfuric Acid and C₈H₁₂O₆ tricarboxylic acid. *Phys. Chem. Chem. Phys.* **2017**, *19*, 4877–4886.

- (33) Elm, J. An Atmospheric Cluster Database Consisting of Sulfuric Acid, Bases, Organics, and Water. *ACS Omega* **2019**, *4*, 10965–10974.
- (34) Besel, V.; Kubečka, J.; Kurtén, T.; Vehkamäki, H. Impact of Quantum Chemistry Parameter Choices and Cluster Distribution Model Settings on Modeled Atmospheric Particle Formation Rates. *J. Phys. Chem. A* **2020**, *124*, 5931–5943.
- (35) Prenni, A. J.; DeMott, P. J.; Kreidenweis, S. M.; Sherman, D. E.; Russell, L. M.; Ming, Y. The Effects of Low Molecular Weight Dicarboxylic Acids on Cloud Formation. *J. Phys. Chem. A* **2001**, *105*, 11240–11248.
- (36) Ho, K. F.; Lee, S. C.; Ho, S. S. H.; Kawamura, K.; Tachibana, E.; Cheng, Y.; Zhu, T. Dicarboxylic Acids, Ketocarboxylic Acids, α -Dicarbonyls, Fatty Acids, and Benzoic Acid in Urban Aerosols Collected During the 2006 Campaign of Air Quality Research in Beijing (CAREBeijing-2006). *Journal of Geophysical Research* **2010**, *115*, D19312.
- (37) Kinatovski, Z.; Grgić, I.; Veber, M. Characterization of Carboxylic Acids in Atmospheric Aerosols Using Hydrophilic Interaction Liquid Chromatography Tandem Mass Spectrometry. *J. Chromatography A* **2011**, *1218*, 4417–4425.
- (38) Zhang, Y. L.; Kawamura, K.; Watanabe, T.; Hatakeyama, S.; Takami, A.; Wang, W. New Directions: Need for Better Understanding of Source and Formation Process of Phthalic Acid in Aeroross as Inferred from Aircraft Observations over China. *Atmospheric Environment* **2016**, *140*, 147–149.
- (39) He, X.; Huang, X. H. H.; Chow, K. S.; Wang, Q.; Zhang, T.; Wu, D.; Yu, J. Z. Abundance and Sources of Phthalic Acids, Benzene-Tricarboxylic Acids, and Phenolic Acids in PM_{2.5} at Urban and Suburban Sites in Southern China. *ACS Earth and Space Chemistry* **2018**, *2*, 147–158.
- (40) Li, X.; Pavuluri, C. M.; Yang, Z.; He, N.; Tachibana, E.; Kawamura, K.; Fu, P. Q. Large

- Contribution of Fine Carbonaceous Aerosols from Municipal Waste Burning Inferred from Distributions of Diacids and Fatty Acids. *Environ. Res. Commun.* **2019**, *1*, 071005.
- (41) Delhaye, D.; Ouf, F.-X.; Ferry, D.; Ortega, I.; Penanhoat, O.; Peillon, S.; Salm, F.; Vancassel, X.; Focsa, C.; Irimiea, C. et al. The MERMOSE project: Characterization of particulate matter emissions of a commercial aircraft engine. *J. Aerosol. Sci.* **2017**, *105*, 48–63.
- (42) Kleindienst, T. E.; Jaoui, M.; Lewandowski, M.; Offenberg, J. H.; Docherty, K. S. The Formation of SOA and Chemical Tracer Compounds From the Photooxidation of Naphthalene and its Methyl Analogs in the Presence and Absence of Nitrogen Oxides. *Atmos. Chem. Phys.* **2012**, *12*, 8711–8726.
- (43) Fraser, M. P.; Cass, G. R.; Simoneit, B. R. T. Air Quality Model Evaluation Data for Organics. 6. C-3-C-24 Organic Acids. *Environ. Sci. Technol.* **2003**, *37*, 446–453.
- (44) Wang, H.; Zhao, X.; Zuo, C.; Ma, X.; Xu, F.; Sun, Y.; Zhang, Q. A Molecular Understanding of the Interaction of Typical Aromatic Acids with Common Aerosol Nucleation Precursors and their Atmospheric Implications. *RSC Advances* **2019**, *9*, 36171–36181.
- (45) Radola, B.; Picaud, S.; Ortega, I. K.; Ciuraru, R. Formation of Atmospheric Molecular Clusters from Organic Waste Products and Sulfuric Acid Molecules: A DFT Study. *Environ. Sci. : Atmos.* **2021**, *1*, 267–275.
- (46) Glendening, E. D.; Reed, A. E.; Carpenter, J. E.; Weinhold, F. NBO Version 3. 1.
- (47) Chai, J. D.; Martin, H. G. Long-Range Corrected Hybrid Density Functionals With Damped Atom–Atom Dispersion Corrections. *Phys. Chem. Chem. Phys.* **2008**, *10*, 6615–6620.
- (48) Elm, J.; Kristensen, K. Basis Set Convergence of the Binding Energies of Strongly

- Hydrogen-Bonded Atmospheric Clusters. *Physical Chemistry Chemical Physics* **2017**, *19*, 1122–1133.
- (49) Grimme, S. Supramolecular Binding Thermodynamics by Dispersion-Corrected Density Functional Theory. *Chem. Eur. J.* **2012**, *18*, 9955–9964.
- (50) Li, Y. P.; Gomes, J.; Mallikarjun Sharada, S.; Bell, A. T.; Head-Gordon, M. Improved Force-Field Parameters for QM/MM Simulations of the Energies of Adsorption for Molecules in Zeolites and a Free Rotor Correction to the Rigid Rotor Harmonic Oscillator Model for Adsorption Enthalpies. *J. Phys. Chem. C* **2015**, *119*, 1840–1850.
- (51) Frisch, M. J.; Trucks, G. W.; Schlegel, H. B.; Scuseria, G. E.; Robb, M. A.; Cheeseman, J. R.; Scalmani, G.; Barone, V.; Petersson, G. A.; et al., H. N. Gaussian 09, Revision C. 01. Gaussian, Inc. , Wallingford CT, 2016.
- (52) Elm, J.; Myllys, N.; Kurtén, T. What Is Required for Highly Oxidized Molecules To Form Clusters with Sulfuric Acid? *J. Phys. Chem. A* **2017**, *121*, 4578–4587.
- (53) Ortega, I. K.; Kupiainen, O.; Kurtén, T.; Olenius, T.; Wilkman, O.; McGrath, M. J.; Loukonen, V.; Vehkamäki, H. From Quantum Chemical Formation Free Energies to Evaporation Rates. *Atmos. Chem. Phys.* **2012**, *12*, 225–235.
- (54) Leverentz, H.; Siepmann, J.; Truhlar, D.; Loukonen, V.; Vehkamäki, H. Energetics of Atmospherically Implicated Clusters Made of Sulfuric Acid, Ammonia, and Dimethyl Amine. *J. Phys. Chem. A* **2013**, *117*, 3819–3825.

TOC Graphic

